Performance Analysis of Dynamic Wireless Charging System for Electric Vehicles: A Queueing Approach

Bo Sun
The Hong Kong University of Science and Technology
bsunaa@ust.hk

Danny H.K. Tsang
The Hong Kong University of Science and Technology
eetsang@ust.hk

ABSTRACT

Dynamic wireless charging (DWC) has recently been acknowledged as a promising solution to alleviate the range anxiety and long-charging-duration issue of electric vehicles (EVs) on highways. However, modeling and analyzing the DWC system are highly challenging because the system dynamics from both the underlying power system and the transportation system have to be jointly considered, which makes the problem highly complicated. Existing works use either simulation-based methods or oversimplified models, where the influences and interactions of system parameters on the resulting performances cannot be well understood. In this paper, we propose a unified analytical model for the DWC system, which captures the major influencing factors in both the underlying power and transportation systems, based on the $M/G/s/s$ state-dependent queueing approach. We also undertake performance analysis to identify significant trade-offs between different important system parameters for DWC infrastructure planning.

CCS Concepts

•Computing methodologies → Model development and analysis;

Keywords

electric vehicles; dynamic wireless charging; state-dependent queue; performance analysis

1. INTRODUCTION

The increase of electric vehicle (EV) penetration gives rise to an increasing demand for the corresponding public refueling facilities [1]. Meanwhile, various refueling technologies have been proposed and successfully commercialized. In particular, refueling facilities can be mainly divided into four categories: *i*) *EV parking lots* (such as homes, office buildings, and public parking garages) allow EVs to stay for a long charging duration (e.g., several hours), while the charging rates are typically restricted to be low [2]. *ii*) *Fast charging stations* refuel the EVs faster (e.g., 30 minutes) with high charging rates but have limited number of chargers at each location due to the power capacity constraints from the power grid [3]. *iii*) *Battery swapping stations* refuel EVs by replacing depleted batteries with fully-charged batteries but each station is only able to serve limited types of EVs because there is still no universal standard for the batteries of EVs [4]. *iv*) *Dynamic wireless charging (DWC) systems* charge EVs while they are passing through a segment of roads equipped with wireless power transfer (WPT) [5]. Unlike the first three categories that require EVs to stop at the stations and refuel (stop-and-refuel), the DWC system charges the EVs while they are driving along the WPT-enabled road (charge-while-driving). Therefore, a well-planned network of DWC systems can support an unlimited driving range for EVs in the ideal case. Compared to stop-and-refuel, charge-while-driving helps EVs reduce the size of their batteries and the associated cost. Moreover, charge-while-driving solution becomes increasingly attractive and important for EVs on highways because it releases EVs from the stop-and-refuel process during their long-distance inter-city travels [6]. In addition, since the WPT for EVs has been under the standardization in recent years [7], we foresee that the DWC system will be able to provide undifferentiated WPT services for EVs from different brands in the near future.

Despite the advantages of the DWC system for EV drivers, there are economical and technical challenges from infrastructure planning and operation for the DWC system. Firstly, the construction cost of the DWC system is extremely high because not only the roads need to be rebuilt to install the wireless chargers beneath [7][8], but additional power supply infrastructure (e.g., transformers and cables) is also required to upgrade the power capacity for the DWC system [9]. From the technical perspective, it is difficult to evaluate the performance of the DWC system because the system parameters, such as the average speed of EVs, are load-dependent due to the traffic congestion on the WPT-enabled roads. Additionally, the analysis needs to take into account all the limitations from the power grid, EV traffic, and the DWC infrastructure. For example, the capacity of the DWC system is restricted by the power congestion (i.e., insufficient power capacity), the traffic congestion (i.e., slowdown of the vehicle speed) and the length of the WPT-enabled road. Furthermore, the DWC system has low flexibilities to optimize the charging operations of EVs [10]. This is because the charging service must be provided promptly while the EV is on

e-Energy '17, May 16–19, 2017, Shatin, Hong Kong

DOI: http://dx.doi.org/10.1145/3077839.3077849

top of the WPT-enabled road. Therefore, the DWC operator loses the capability of shifting the EV charging demand over time, namely, the deferrable property, to control the charging process. Moreover, a relatively high charging rate is required for each EV so that it can receive a substantial amount of energy from the DWC system.

In this paper, we focus on steady-state performance analysis of the DWC system based on analytical models. Our contributions are three-fold. First, we propose to model the DWC system as an $M/G/s/s$ state-dependent queue. The coupling of the transportation system, power system and DWC system is shown explicitly by determining the parameters of the queueing model. Second, steady-state analysis is performed on the EV traffic and the power consumption. Analytical results are derived based on the proposed queueing model. Third, by evaluating the performance of the DWC system under various power and transportation system conditions, we identify and discuss the important factors for improving the system performance and the opportunities for revenue maximization in the short-term operation. In addition, different layout designs of the WPT-enabled road are analyzed and compared, and useful insights are provided for the long-term infrastructure planning based on the proposed queueing model.

2. RELATED WORKS

Although the concept and principles of WPT can date back to the pioneering work by Nikola Tesla century ago, applying WPT to the highways just draws the attention from the industry and academy in recent years. At this initial stage, the first stream of studies focus on validating the feasibility of the DWC system. Many research entities, such as the Highways England [6], Oak Ridge National Laboratory (ORNL) [7] and the Korea Advanced Institute of Science and Technology (KAIST) [8], have developed prototypes of the DWC system to study the effectiveness and efficiency of the WPT for EVs. It has been demonstrated that a high efficiency of $70-80$ percent at more than 50 kW charging rate can be achieved between the chargers buried beneath the road and the receivers equipped by the EVs [7][11].

In the literature on performance evaluation of the DWC system, the core difficulty is how to model the EV traffic on the WPT-enabled road. [9] proposes to use mesoscopic approach to simulate the road traffic and assess the energy consumption of the DWC system accordingly. [12] integrates the road traffic simulation into the power flow analysis of the power system and investigates the impact of EV traffic on the power flow and voltage of the power grid. Although simulation-based methods can evaluate the performance of the DWC system when all the system parameters are given, the influences and interactions of these parameters on the resulting performances cannot be well understood. Thus, analytical models and their corresponding analysis for the DWC system are desired for optimizing the operations and planning the infrastructure of the DWC system. Recent works [13] and [14] propose to model the DWC system as an $M/G/\infty$ queue and an $M/M/s$ loss queue, respectively. Although these two queueing models are easy to analyze, they ignore the road traffic congestion, which is the key characteristic of the DWC system. In particular, it is assumed that each EV can drive at a constant speed on the WPT-enabled road [13][14] and this speed can be controlled directly by the DWC operator [14]. However, these two assumptions are both impractical. First, in the transportation traffic engineering, the speed of vehicles on the road is non-increasing in the vehicular density (i.e., number of EVs for a fixed length of the road). Thus, the traffic congestion on the WPT-enabled road may greatly affect the service time and hence has to be taken into account. Secondly, it is impractical for the DWC operator to control the speed of all the vehicles unless all the EVs are enabled autonomous driving. A realistic case is to decide the posted speed limit of the road. However, under different traffic conditions, the realized speeds of vehicles on the road may deviate far from the speed limit.

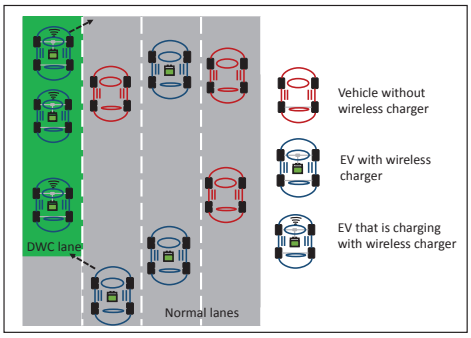

Figure 1: Illustration of the DWC system on highways.

3. A STATE-DEPENDENT QUEUEING MODEL FOR THE DWC SYSTEM

Consider the DWC system on highways as shown in Fig. 1. A segment of one lane from the highway is rebuilt to enable the wireless charging capability. Let L denote the length of the WPT-enabled road. All EVs, which are driving along the WPT-enabled road, are charged with the same constant charging rate r. For simplicity of presentation, EVs in this section refer to the EVs that have charging requests and have been equipped with wireless chargers. We assume that the communication has been established between the EVs and the DWC operator by technologies such as cellular network or dedicated short-range communication. When an EV approaches the entrance of the DWC system, it submits a request for entering the DWC system, and then the DWC operator decides whether this EV can be admitted to enter the system based on its available capacity s. The admitted EVs start to charge immediately after they enter the WPT-enabled road, and receive the charge-while-driving service until reaching their energy requirement or driving to the end of the WPT-enabled road. The rejected EVs are considered to be blocked by the DWC system and can resort to other nearby refueling systems. Note that EVs are not allowed to enter but can leave the DWC system in the middle of the WPT-enabled road. This restriction is a simplification of the real model and can be relaxed by considering more complex models. Details of this simplification are discussed in Remark 2.

3.1 An M/G/s/s State-dependent Queue

The DWC system is modeled as an $M/G/s/s$ queue with state-dependent service rates. Particularly, the EVs with wireless charging requests are the customers of the DWC system. As shown in Fig. 2 based on the measured data in

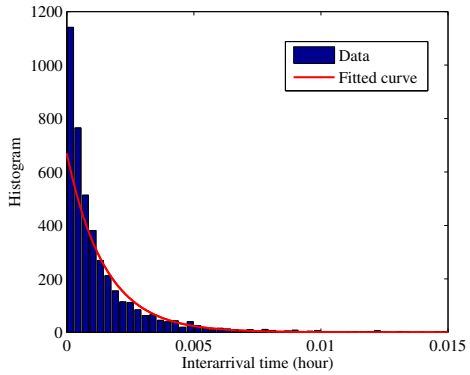

Figure 2: Illustration of the histogram of the interarrival time of vehicles that enter Decoto Rd. from 10 am to 5 pm. The interarrival time distribution can be approximated by an exponential function with an average rate 670 EVs/hour.

[15], these EV arrivals are assumed to follow the Poisson arrival process with an average rate λ. The WPT-enabled road is modeled as s parallel servers, which basically means at most s EVs are allowed to drive and charge simultaneously on the WPT-enabled road. $0 \leq s \leq c$ is the available capacity determined by the DWC operator and c is the capacity of the DWC system. Any arrival that finds all s servers busy is blocked. The service time for each EV is the time period during which EV drives on the WPT-enabled road. Therefore, the service time directly depends on the speed of EVs in the DWC system. In order to take into account the traffic congestion on the WPT-enabled road, we model the average speed of EVs to be state (i.e., the number of EVs) dependent. Thus, the service time of the $M/G/s/s$ queue is state-dependent as well. Denote by $\mu(n), n = 1, \ldots, s$ the average service rate when n EVs are driving on the WPT-enabled road. Based on [16][17], the steady-state probabilities of a state-dependent $M/G/s/s$ queue are expressed as follows,

$$p_n = \frac{\lambda^n}{n! \Pi_{m=1}^{n} \mu(m)} p_0, \tag{1}$$

where $p_0 = \left[1 + \sum_{n=1}^{s} \frac{\lambda^n}{n! \Pi_{m=1}^{n} \mu(m)}\right]^{-1}$. Note that when the average service rates are not state-dependent, namely $\mu(n) = \mu$, Eq. (1) reduces to the Erlang B formula for the $M/G/s/s$ loss system with the i.i.d service time distribution. It can be observed that the steady state distribution of the $M/G/s/s$ state-dependent queue depends on the average arrival rate λ, the available capacity s and the average service rates $\mu(n)$. Given a fixed λ, both s and $\mu(n)$ are determined by the parameters from the transportation system, power system, and DWC system. Before going into the specifications of these parameters, we address the advantages and relationship of the proposed state-dependent queue with other similar queueing models.

Remark 1. The proposed $M/G/s/s$ state-dependent queue has the following advantages for modeling the DWC system: *i*) (insensitivity) The steady-state probabilities only depend on the means of the service time distribution and can be calculated by efficient algorithms based on this property. *ii*) The departure process is also Poisson process. This property facilitates a natural extension to analyze a network of DWC systems.

Remark 2. The state-dependent queueing model is a trade-off between the practice and theory. Recall that we assume that EVs are only admitted to enter the DWC system at the entrance. However, other admission rules may be more practical. For example, EVs may be allowed to enter the DWC system at any position alongside the WPT-enabled road as long as the instantaneous number of EVs on the road is smaller than the available capacity. In this case, the rejected EVs with charging requests keep driving on the normal lanes alongside the charging lane, and are considered in the waiting buffer of the DWC system. Furthermore, these EVs in the buffer will be abandoned once they pass through the end of the DWC system. Under this admission rule, the DWC system can be modeled as a state-dependent $M/G/s/d+G$ queueing model, where d is the total capacity including the buffer and the second G represents that the EVs in the buffer will be abandoned from the system following a general distribution. However, the performance of this queueing model is much more difficult to evaluate. The other extreme case is that we assume the $M/G/s/s$ queue is state independent, which means that service time follows i.i.d general distribution. In this case, the model is reduced to the Erlang B model, which possesses various nice theoretical properties. However, the Erlang B model ignores the impact of traffic congestion on the speed of EVs, which oversimplifies the practical system. Thus, in order to model the DWC system with tractable solution methods and practical features, we choose the $M/G/s/s$ state-dependent queueing model.

3.2 Capacity of the DWC System

The available capacity s is an operational parameter, which is decided by the DWC operator for admission control of the DWC system. However, s cannot be arbitrarily large because it is upper-bounded by the capacity of the DWC system. The capacity c is the maximum number of EVs that can be accommodated simultaneously by the DWC system. This capacity is decided by both the power capacity and traffic capacity. Particularly, due to the limited power supply of the power grid, the maximum number of EVs in the DWC system is restricted to be lower than $c_p = \lfloor C_p/r \rfloor$, where C_p is the power capacity and $\lfloor x \rfloor$ denotes the largest integer less than x. Note that C_p is the maximum available power supply to the DWC system. The setting of C_p is determined to optimize the reliability and efficiency of the power grid in the infrastructure planning stage. In order to derive the traffic capacity, we start from the basic relationship among the traffic flow, speed and density. The EV traffic flow on the WPT-enabled road is determined by $\theta = \rho v$, where ρ is the EV density (i.e., average number of EVs per unit distance) and v is the average speed. Moreover, the average speed of all the EVs on the WPT-enabled road is a function of the EV density and the upper speed limit u, namely,

$$v = g(\rho, u), \tag{2}$$

where $\underline{u} \leq u \leq \overline{u}$ is the upper speed limit (or simply speed limit) of the WPT-enabled road [16][18]. In the transportation traffic engineering [22], $g(\rho, u)$ is non-increasing in ρ because a larger ρ indicates a smaller distance between two EVs and thus requires a lower safety speed. $\underline{u}$ and $\overline{u}$ are the minimum and maximum speed limits, respectively. u is decided by the DWC operator to optimize the system performance such as safety and efficiency. Define the jam den-

Table 1: Function forms of speed-density relationship

Model	Function forms	Parameters
Linear	$v(n) = u \times (1 - \frac{n-1}{\alpha_1})$	u, α_1
Exponential	$v(n) = u \times \exp(-(\frac{n-1}{\alpha_1})^{\alpha_2})$	u, α_1, α_2
Two-regime	$v(n) = \begin{cases} u(1 - \frac{n-1}{\alpha_1}), & n < n_1 \\ u_1(1 - \frac{n}{\alpha_2}), & n \geq n_1 \end{cases}$	α_1, α_2, u, u_1, n_1

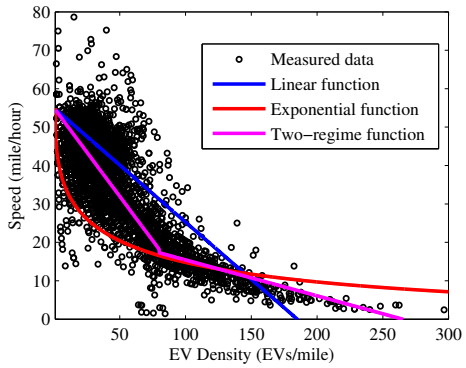

Figure 3: Illustration of the speed-density relationship.

sity of the WPT-enabled road by $\overline{\rho}$, for which $g(\overline{\rho}, u) = 0$. In this case, the traffic flow is zero, which means that the WPT-enabled road is too congested to admit additional EVs. Therefore, the traffic capacity is expressed as $c_t = \lfloor \overline{\rho} L \rfloor$. Based on empirical studies, the jam density $\overline{\rho}$ varies under different testing conditions and can be approximated in the range of $185 - 265$ veh/mile/lane [22]. However, for a practical setting of the DWC system on highways, a lower speed limit $\underline{v}$ is also posted to ensure that the vehicles can at least drive at a speed of $\underline{v}$. For example, speed limit of highways in the U.S. is required not to be below 35 miles/hour, which is the same value as the speed limit in the urban areas. In this case, the limit density $\overline{\rho}(\underline{v})$ satisfies $g(\overline{\rho}(\underline{v}), u) = \underline{v}$ and the traffic capacity is $c_t = \lfloor \overline{\rho}(\underline{v}) L \rfloor$. In summary, the capacity of the DWC lane is

$$c = \min\{c_p, c_t\}. \tag{3}$$

The capacity of the DWC system is decided in the infrastructure planning stage and is typically set to be large enough to accommodate various EV traffic. Moreover, we find the speed limit u is also a controllable parameter for the DWC operator. Once u is set, the average speed of EVs is purely decided by the instantaneous EV density.

3.3 State-dependent Service Rates

Recall that the service time depends on the charging time to reach the target energy requirement and the driving time to drive through the DWC system. Both charging time and driving time depend on the speeds of the EVs, which are determined by the EV density and speed limit as shown in Eq. (2). Thus, in the following, we first show the method of deriving the speed-density relationship for a given speed limit based on the empirical model and measured data, and then derive the state-dependent service rates.

3.3.1 *Speed-density Relationship for Road Traffic*

Let $v(n) = g(n/L, u)$ denote the average speed when n EVs drive on the WPT-enabled road given fixed road length L and speed limit u. In the literature, various deterministic or stochastic models [18][19] have been proposed to capture the relationship of density and speed by fitting the empirical data. Based on these empirical studies, we can approximate the average speed $v(n)$ as a deterministic function of n with scenario-dependent parameters. Some well-recognized approximation functions are listed in Tab. 1 [18]. One common feature of these functions is that the average speed has a non-increasing relationship in the number of EVs.

Fig. 3 shows an example of the speed-density relationship. The measured data are collected at the location Decoto Rd. by loop detector [15]. The parameters of the linear, exponential and two-regime functions are estimated by curve fitting based on the data. The speed limit is set to be 55 miles/hour in the fitted curves.

Table 2: System parameters

Parameters	Value
Battery capacity	16 kWh
Initial SoC	$\mathcal{N}(0.3,0.15,0.05,0.8)$
Target SoC	0.9
Length of lane L	10 miles
Driveline efficiency η_d	1
Ancillary power r_a	0.8 kW
Power transmission rate r	50 kW
Wireless charging efficiency η_c	0.75
Resistance to motion ξ	0.227 kWh/mile

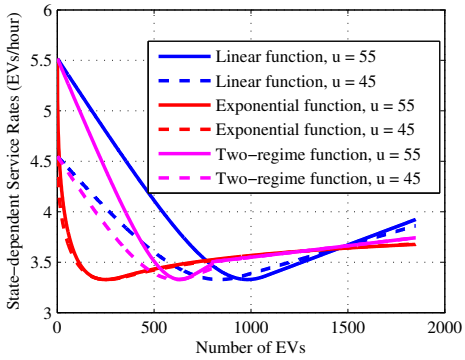

Figure 4: State-dependent service rates with different speed-density function forms and speed limits.

3.3.2 *Service Time Distribution*

Given that n EVs are driving on the WPT-enabled road at an average speed of $v(n)$, the driving time is denoted by

$$t_d(n) = \frac{L}{v(n)}. \tag{4}$$

For the EVs with energy requirement E, the charging time can be determined by

$$t_c(n) = \frac{E}{r\eta_c - \xi v(n)/\eta_d - r_a}, \tag{5}$$

where $r\eta_c - \xi v(n)/\eta_d - r_a$ is the net charging rate of the DWC system. Particularly, r is the constant charging rate transmitted from the WPT-enabled road and η_c is the efficiency of WPT. Thus, $r\eta_c$ denotes the effective charging rate that

each EV receives. $\xi v(n)/\eta_d + r_a$ is the energy consumption rate when the EVs drive at a speed of $v(n)$. Specifically, ξ is the resistance to motion, which quantifies the energy consumption rate per unit of speed [9][14]. η_d is the driveline efficiency. r_a is the energy consumption rate that is not related to EV motion such as lighting and air conditioning. All the parameters in the net charging rate are independent of the speed $v(n)$. Combining Eq. (4) and Eq. (5), the service time is determined by

$$t(n) = \min\{t_c(n), t_d(n)\}. \tag{6}$$

Thus, the state-dependent average service rate with n EVs on the WPT-enabled road is $\mu(n) = 1/\mathbb{E}[t(n)]$.

Fig. 4 illustrates the state-dependent service rates under different speed-density function forms and speed limits. System parameters are listed in Tab. 2. In order to estimate the distribution of the energy requirement E, we assume that all the EVs have the same battery capacity and have the same target state-of-charge (SoC). In addition, when the admitted EVs enter the DWC system, their initial SoC follows the same truncated normal distribution. In Fig. 4, it can be observed that all the state-dependent service rates have similar trends under different scenarios. In the fast speed regime (i.e., the region with a small number of EVs), the service rate decreases as the increase of the number of EVs because in this regime, most of the EVs are unable to charge to the target SoC before it reaches the end of the WPT-enabled road. Therefore, their service time is dominated by the driving time $t_d(n)$ and the service rate decreases as the increase of the number of EVs. When the speed of the EVs is further reduced below a certain threshold (i.e., the number of EVs increases above some threshold), the net charging rate increases to a large enough value. In this case, the service time is dominated by the charging time $t_c(n)$. The service rate increases gradually with the decrease of the speed as the result of the increase in the number of EVs as shown in Fig. 4. In addition, it can be observed that in the fast speed regime, the service rates under high speed limits are much higher than those under low speed limits. However, in the slow speed regime, the service rates under different speed limits are close. This indicates that the control of the speed limit can be more effective when the system is in the fast speed regime.

3.4 Performance Metrics

After the derivation of the capacity and the state-dependent service rates, the steady-state probabilities of the number of EVs in the DWC system can be determined based on Eq. (1). Although the steady state probabilities have closed form expressions, numerical calculation for large available capacity s (e.g., hundreds or thousands) will encounter severe overflow issues and rounding errors [20] because p_n involves large powers and factorials. Thus, we propose to calculate the steady-state probabilities by Alg. 1, which is based on the general recursive approach to calculate the stationary probabilities of birth-death process in [20]. The key idea is to put the normalization step inside the for loop, which can avoid the numerical overflow at the expense of higher computational complexity. Then, important performance metrics of the DWC system can be calculated accordingly.

3.4.1 Blocking Probability

Given the available capacity s and speed limit u, the blocking probability is

$$B(s,u) = p_s = \frac{\lambda^s}{s!\Pi_{m=1}^{s}\mu(m)} p_0. \tag{7}$$

Observing the similarity between $B(s,u)$ and the Erlang B loss formula, the calculation of $B(s,u)$ can be further simplified into the following recursive equation, which is a generalization of the recursive approach to compute the Erlang B loss probability,

$$B(s,u) = \frac{\lambda B(s-1,u)}{s\mu(s) + \lambda B(s-1,u)}, \quad s = 1,2,\ldots, \tag{8}$$

and $B(0,u) = 1$. The derivation of Eq. (8) is as follows. Firstly, $B(0,u) = 1$ is clear because no server means all the customers are blocked. Based on Eq. (7), we have

$$\frac{1}{B(s,u)} = \frac{1 + \sum_{n=1}^{s} \frac{\lambda^n}{n!\Pi_{m=1}^{n}\mu(m)}}{\frac{\lambda^s}{s!\Pi_{m=1}^{s}\mu(m)}} \tag{9}$$

$$= \frac{1 + \sum_{n=1}^{s-1} \frac{\lambda^n}{n!\Pi_{m=1}^{n}\mu(m)} + \frac{\lambda^s}{s!\Pi_{m=1}^{s}\mu(m)}}{\frac{\lambda^s}{s!\Pi_{m=1}^{s}\mu(m)}} \tag{10}$$

$$= \frac{s\mu(s)}{\lambda} \frac{1 + \sum_{n=1}^{s-1} \frac{\lambda^n}{n!\Pi_{m=1}^{n}\mu(m)}}{\frac{\lambda^{s-1}}{(s-1)!\Pi_{m=1}^{s-1}\mu(m)}} + 1 \tag{11}$$

$$= \frac{s\mu(s)}{\lambda B(s-1,u)} + 1. \tag{12}$$

Then, we have the recursion expression (8).

The blocking probability indicates the proportion of EVs that cannot be served by the DWC system and hence represents the quality of service (QoS) of the DWC system. In order to provide good services for the customers, DWC operators need to ensure the blocking probability under a certain threshold.

Algorithm 1 Computing the Steady-state Probability of the $M/G/s/s$ Queue with State-dependent Service Rates

Input: Number of servers s, average arrival rate λ, and state-dependent service rates $\mu(n)$, $n = 1,2,\ldots,s$.
Output: Steady-state probabilities p_n, $n = 0,1,\ldots,s$.
Initialize $p_0 = 1$.
for $n = 1$ **to** s **do**
  $p_n = \frac{\lambda}{n\mu(n)} p_{n-1}$;
  $\Sigma = 1 + p_n$;
  $p_m = p_m/\Sigma$, $m = 0,1,\ldots,n$;
end for

3.4.2 Carried Load

The carried load, which is the average number of EVs in the DWC system, can be calculated by

$$N(s,u) = \sum_{n=1}^{s} p_n n. \tag{13}$$

Because each EV is charged at the same charging rate, $N(s,u)$ reflects the total energy transfer from the DWC system per time unit. When the DWC system makes profits by selling electricity to the EVs, $N(s,u)$ indicates the capability of the system to generate profits.

3.4.3 Average Transferred Energy per EV

If a fixed amount of energy is transferred from the DWC system to EVs, the energy may be transferred to either a small number of EVs with adequate individual received energy or many EVs, each of which receives only a small portion of the total energy. Although these two cases make no differences to the DWC operator, EVs receive totally different services. Thus, we propose to capture this performance by the average transferred energy per EV, which is calculated by

$$T(s,u) = \mathbb{E}[W] \sum_{n=1}^{s} p_n(r\eta_c - \xi v(n)/\eta_d - r_a). \quad (14)$$

where $\mathbb{E}[W] = N(s,u)/\lambda(1 - B(s,u))$ represents the average service time based on Little's law. In order to provide good services, a service-level agreement is needed to quantify the average transferred energy that the DWC system provides for each EV. Moreover, to maintain a fixed $N(s,u)$, the DWC operator needs to decide whether to block more EVs to guarantee $T(s,u)$ or admit more EVs to guarantee $B(s,u)$. This trade-off will be shown and discussed in details in the next section.

4. PERFORMANCE EVALUATION AND DISCUSSIONS

In order to improve the performance of the DWC system, the DWC operator needs to take into account both the short-term operational parameters and the long-term infrastructure parameters. According to the vehicular traffic condition in the short run, the available capacity s and the speed limit u can be conveniently controlled by DWC operators to optimize the revenue-related or QoS-related performance metrics. In contrast, the infrastructure parameters (e.g., the length L and the charging rate r of the DWC system) typically will not change for years once the infrastructure is constructed. However, the infrastructure parameters are not designed for a fixed EV traffic condition because on the one hand, the highway traffic varies with time within one day. While on the other hand, the EV penetration changes from year to year, and hence the traffic condition changes gradually. These changes in the EV traffic may degrade the system performance significantly if the DWC operator has too limited operational opportunities when facing different traffic conditions under the same infrastructure parameters. Thus, in the long run, the infrastructure parameters need to take into account both the construction cost and the flexibilities of short-term operations based on the prediction of EV arrivals in the future.

In this section, we first show the effectiveness of the short-term operational parameters on the system performance and illustrate the operational flexibility in the short run based on a QoS-guaranteed revenue maximization problem. Afterwards, we investigate the trade-offs in the long-term parameters in the infrastructure planning of the DWC system.

4.1 Impact of Short-term Parameters

In this section, we consider that the DWC system has already been built and the long-term parameters are fixed. We aim to study how the short-term parameters, namely, the available capacity s and the speed limit u affect the performance of the DWC system and to provide insights for the DWC operator to perform admission control and speed regulation.

Fig. 5 illustrates the impact of the available capacity s and speed limit u on the blocking probability $B(s,u)$, carried load $N(s,u)$ and average transferred energy $T(s,u)$ under different traffic conditions. The lower bound of the speed limit is set to be 0 and other system parameters are listed in Tab. 2. In the light and moderate traffic conditions which are presented by triangle and circle markers respectively, three important messages are conveyed. First, we can see the three performance metrics are improved as the increase of the available capacity s until s exceeds a certain value. Therefore, in order to achieve the best performance, the available capacity is not necessarily to be chosen as the capacity of the DWC system. Second, the speed regulation has a controversial impact on the blocking probability and the carried load. From the DWC operator's perspective, a larger carried load typically means higher profit opportunity and a larger blocking probability means a bad service. Thus, the DWC operator expects the system to be operated with a high carried load and a low blocking probability. However, the increase of the speed limit reduces both the blocking probability and the carried load of the DWC system. Thus, the setting of the speed limit is non-trivial. Third, when the DWC system is transferring the energy at the high power rate, it does not mean the individual EV can receive enough energy after passing through the DWC system. The reason is as stated in the previous section, the total transferred energy can either be divided by a small number of EVs with high $T(s,u)$ or be shared by a large number of EVs but each of them only receives a small amount of energy. As can be seen from the curves with low available capacities in Fig. (5b), all these cases have the same carried load. However, blocking probabilities and average transferred energy of these cases are differentiated by speed limits and traffic conditions. The DWC operator needs to decide whether to provide high energy for admitted EVs by sacrificing blocking probability, or to serve as many EVs as possible by bearing possible low transferred energy per EV. A trade-off between these factors needs to be further explored. Thus, QoS of the DWC system is defined by both the blocking probability and the average transferred energy.

Although the observations in the light and moderate traffic cases are as expected, the results do not necessarily hold in the heavy traffic case which is shown by the black curves with cross markers. For example, the trade-off between the blocking probability and the carried load is not that significant when the available capacity is large enough. In this case, increasing the speed limit can raise the carried load without affecting the blocking probability. The reason for this unexpected result is due to the state dependence of the service rates, which change with the increase of EV traffic. As shown in Fig. 4, the service rates in the low speed limit case (e.g., the dashed blue line) surpass these in the high speed limit case (e.g., the solid blue line) when the traffic is intensive (i.e., around 1000 EVs).

In many cases, when we discuss the control of speed limits, we only consider the upper speed limit. However, the lower speed limit is also important to avoid traffic congestion on the road. In fact, the lower speed limit is included in the decision of the available capacity because the average speed of the EVs is non-increasing in the number of EVs in the system. When a lower speed limit is set, the upper bound of available capacity is determined accordingly. Fig. 6 illustrates the impact of the lower speed limit. Particularly, all

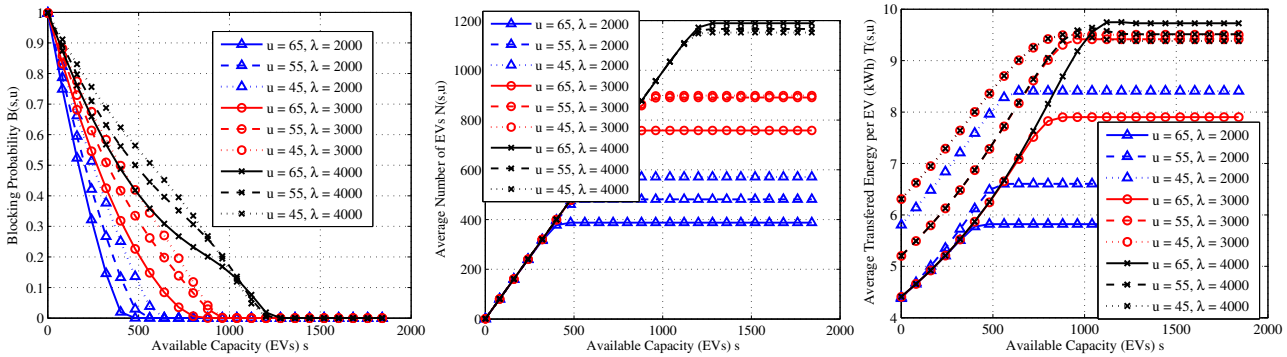

(a) Blocking probability (b) Average number of EVs (c) Average transferred energy per EV

Figure 5: Illustrating the impact of short-term parameters on the DWC system. No lower speed limit is required.

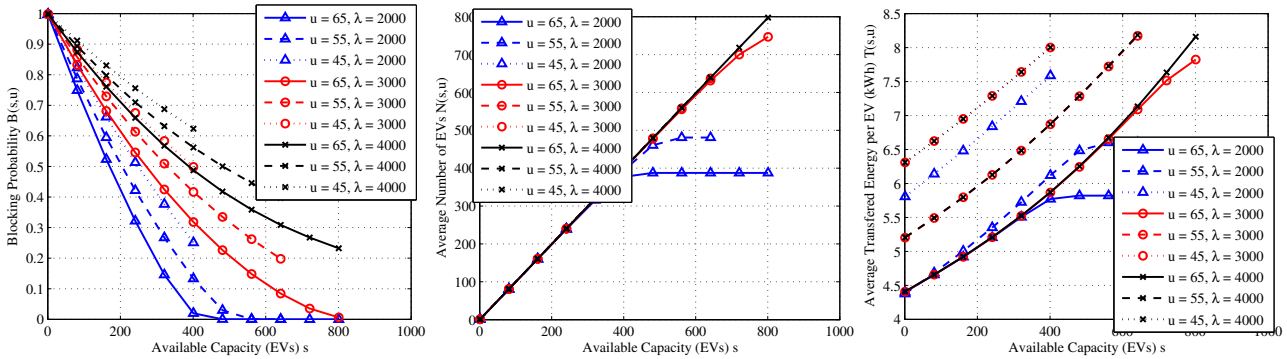

(a) Blocking probability (b) Average number of EVs (c) Average transferred energy per EV

Figure 6: Illustrating the impact of short-term parameters on the DWC system. The lower speed limit is set to be 35 miles/hour.

the parameters of Fig. 6 are set to be the same as those in Fig. 5 but the speed is set to be larger than 35 miles/hour, which is also a common value for the upper speed limit of urban areas. The key observation from Fig. 6 is that the effectiveness of the speed control is reduced significantly after the lower speed limit is imposed. Specifically, in order to guarantee the lower speed limit, the DWC system is only able to utilize a small portion of the whole capacity of the system. Furthermore, with the decrease of the upper speed limit, the upper bound of the available capacity decreases. As shown in Fig. (6b), the carried load is nearly not affected by the upper speed limit in the moderate and heavy traffic conditions. This phenomenon greatly restricts the capability of the DWC operator to decide the trade-off between blocking probability and carried load in the heavy traffic cases.

4.2 Revenue Model and QoS

As shown in the last subsection, given the EV traffic and infrastructure parameters, the performance metrics of the DWC system depend on the available capacity s and the speed limit u, which can be controlled by the DWC operator to optimize its revenue and QoS. In particular, the revenue of the DWC system within a time duration of τ can be defined as

$$R(s,u) = rN(s,u)\tau(q_c - q_e) - f_\tau(sr), \tag{15}$$

where q_c is the DWC service price charged to EVs in the unit of \$/kWh, q_e is the electricity price from the power grid and $f_\tau(\cdot)$ is the peak power cost function of the whole time duration τ. The first term of (15) denotes the profits by transferring an amount of energy $rN(s,u)\tau$. The second term denotes the peak power cost when s is chosen as the available capacity. Note that $rN(s,u)\tau$ is the transmitted energy from the DWC system because the EVs are considered to pay for the power loss through the WPT.

Besides maximizing the revenue by providing WPT services, the DWC system operator also needs to understand and guarantee its QoS as a service provider. Thus, for the DWC operator, a joint admission control and speed regulation problem to maximize its revenue with QoS guarantee can be formulated as

$$\max_{s,u} \quad R(s,u) \tag{16}$$

$$\text{s.t.} \quad B(s,u) \le \varepsilon, \tag{17}$$

$$T(s,u) \ge e, \tag{18}$$

$$1 \le s \le c, \quad \underline{u} \le u \le \overline{u}. \tag{19}$$

where ε and e are the blocking probability threshold and

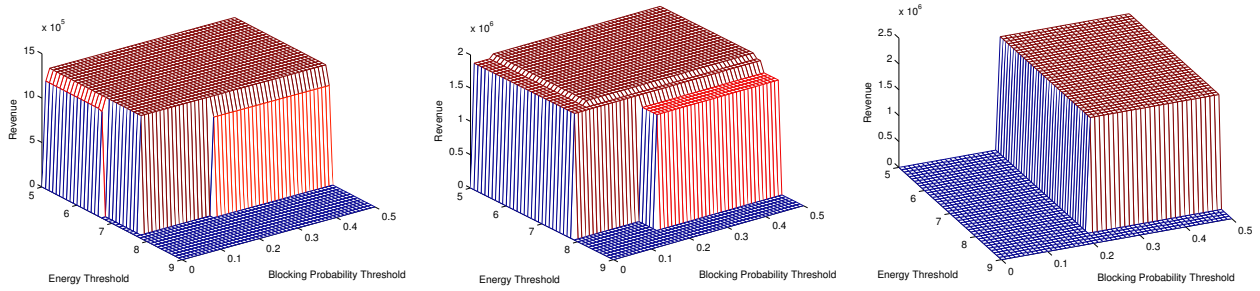

(a) EV arrival rate $\lambda = 2000$ EVs/hour (b) EV arrival rate $\lambda = 3000$ EVs/hour (c) EV arrival rate $\lambda = 4000$ EVs/hour

Figure 7: Illustration of the maximum revenue under different blocking probability and average transferred energy requirements.

energy threshold, respectively. They are predetermined by the DWC operator to guarantee its QoS. In the U.S., the speed limit on highways is required not to be lower than $\underline{u} = 35$ miles/hour. In addition, the speed limit typically increases by 5 miles/hour each time up to $65-70$ miles/hour. Thus, the search space of the speed limit only contains $7-8$ discrete values. As for the available capacity, we have $s \leq c \leq c_t = \lfloor \overline{\rho} L \rfloor$. For the WPT-enabled road with a length of 10 miles, the size of the search space for s is no larger than 2650. Thus, the problem (16) can be solved by brute force search over s and u without much effort.

Fig. 7 shows the maximum revenue with different blocking probabilities and average transferred energy requirements. The average EV arrival rates are set to be $\lambda = 2000$, $\lambda = 3000$ and $\lambda = 4000$ EVs/hour in Figs. (7a) - (7c), respectively. The charging price is set to be $q_c = 0.1$ \$/kWh. Based on the electricity tariff in [21], the energy price is $q_e = 0.0837$ \$/kWh. In addition, the peak power cost function is $f_\tau(sr) = q_p sr$ with a time duration of half a year and the peak power price is $q_p = 19.27$ \$/kW. By calculating the maximum revenue when the energy requirement is changed in the range of $[5.0, 9.0]$ kWh and the blocking probability requirement varies in $[0, 0.5]$. It can be observed that the revenue of the DWC system can be maximized by setting the blocking probabilities larger than ε^* and the energy requirement to be smaller than e^* kWh. For example, $\varepsilon^* = 0.02$ and $e^* = 7.7$ can numerically be obtained in Fig. 7a. More importantly, ε^* and e^* quantify the operational flexibility of the DWC system. A smaller ε^* and a larger e^* indicate that the DWC operator can guarantee the QoS more easily without sacrificing its maximum revenue by choosing s and u as the optimal solution of problem (16). It can also be observed that the operational flexibility decreases as the increase of the EV traffic by comparing Figs. (7a) - (7c). Especially, ε^* becomes rather large in the heavy traffic case, which means the system cannot guarantee the blocking probability to be a small value. This fact is also shown in Fig. (6a). Thus, the infrastructure parameters are not appropriate for accommodating the traffic condition with an average EV arrival rate of $\lambda = 4000$.

4.3 Trade-offs in Long-term Parameters

In this section, we mainly investigate two important parameters in the infrastructure planning of the DWC system, namely, the road length L and the charging rate r of the DWC system. In the following, we evaluate the performance of three possible types of layouts of the DWC system, which have the same construction cost but different values of road length and charging rate. By comparing these three layouts, we aim to understand the trade-offs in choosing the long-term infrastructure parameters. Assuming that there is a budget to build a WPT-enabled road with a length of L and charging rate r, we have three possible layouts for the design of the WPT-enabled road as shown in Fig. 8.

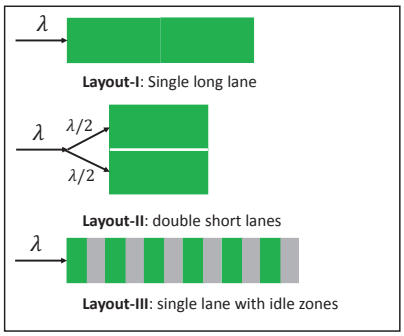

Figure 8: Illustration of three types of layouts for the DWC system.

- **Layout-I:** Single long lane with a length of L and charging rate r.
- **Layout-II:** Double short lanes, each of which has a length of $L/2$ and charging rate r. The arrival traffic splits equally into the two short lanes. EVs are not allowed to change lanes in the WPT-enabled roads.
- **Layout-III:** Single long lane with idle zones. The charging and idle zones are deployed alternately. For the idle zone with a total length of I, the length of the WPT-enabled road is $L + I$ with an average charging rate $\frac{L}{L+I} r$.

4.3.1 *Comparison of* Layout-I *and* Layout-II

According to our proposed queueing model, **Layout-I** is an $M/G/s/s$ state-dependent queue while **Layout-II** can be modeled as two separate queues, each of which has $s/2$

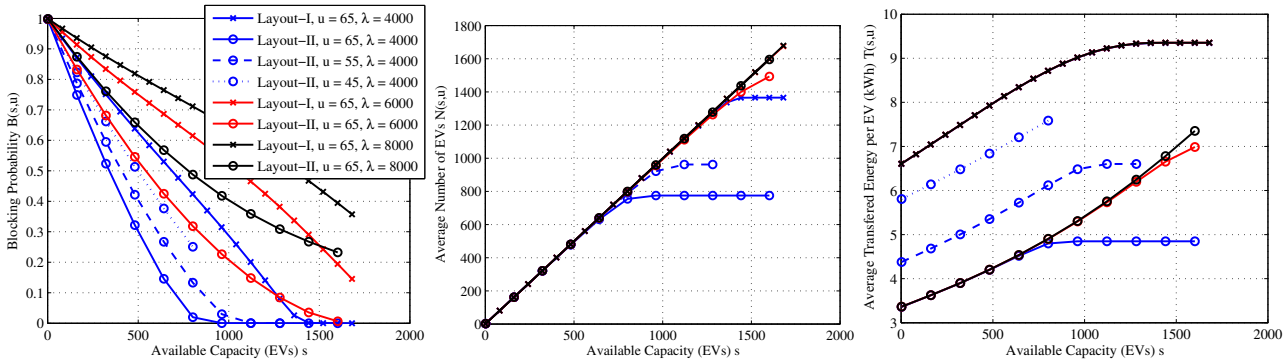

(a) Blocking probability (b) Average number of EVs (c) Average transferred energy per EV

Figure 9: Comparison of **Layout-I** and **Layout-II**.

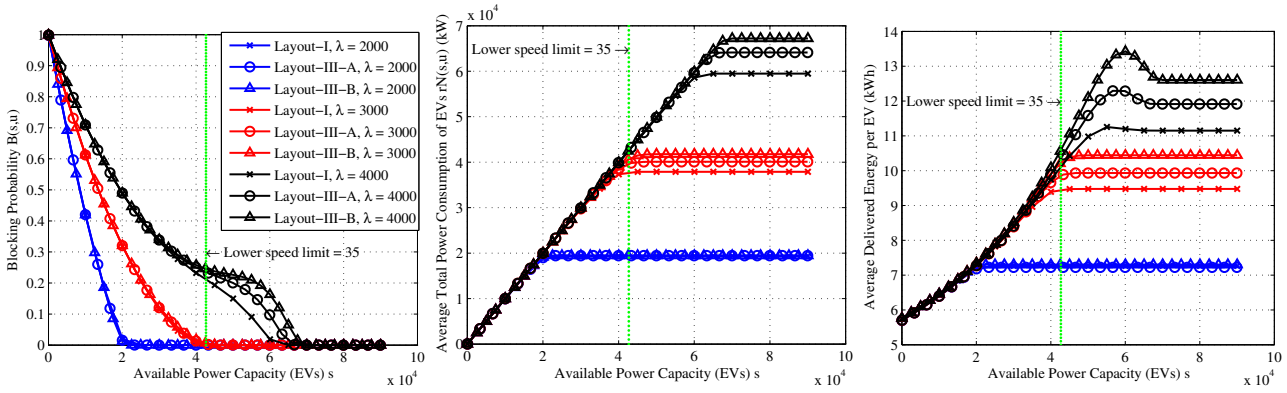

(a) Blocking probability (b) Average total power consumption (c) Average delivered energy per EV

Figure 10: Comparison of **Layout-I** and **Layout-III**.

servers. **Layout-I** is equivalent to combining all the servers of **Layout-II** together and forming a big queue. If the service rates do not depend on the number of EVs and the road length of the DWC system, **Layout-I** is known to perform better compared to **Layout-II** because the service multiplexing of **Layout-I** can avoid the waste of idle servers in **Layout-II**. However, when the state-dependent service rates are considered, the performance of the system also heavily depends on the EV arrival rate. The small queue of **Layout-II** faces a small EV traffic which improves its service rates. Meanwhile, each small queue has faster service rates than the big queue due to its short length. Thus, there is no absolute answer on which layout is better.

Fig. 9 illustrates the performance of the two layouts under different traffic conditions. We set $L = 20$ miles and $r = 50$ kW for the long lane of **Layout-I**, and $L = 10$ miles and $r = 50$ kW for each of the short lanes of **Layout-II**. A lower speed limit of 35 miles/hour is restricted. Roughly speaking, **Layout-II** has lower blocking probabilities but has lower carried load and average transferred energy compared to **Layout-I**. Particularly, in the moderate and heavy traffic cases, the carried loads of **Layout-I** and **Layout-II** are relatively close to each other. However, they have opposite performances in blocking probabilities and average transferred energy. In the light traffic case, the performance of **Layout-II** under different speed limits is shown. It can be observed that higher average transferred energy can be achieved by controlling the speed limit and sacrificing the blocking probability. However, there is no opportunity for **Layout-I** to control the speed limit to reduce the blocking probability because the speed limit has already been set to be the maximum value. From this point of view, **Layout-II** is superior to **Layout-I** because the DWC operator can have more opportunities to operate the system under different traffic conditions to optimize the system performance.

4.3.2 *Comparison of* **Layout-I** *and* **Layout-III**

From the result of the last subsection, a long lane generally outperforms two short lanes in average transferred energy but underperforms in blocking probability. In this section, we aim to investigate whether **Layout-III**, which extends the length of the charging lane by sacrificing its charging rate, can help improve the average transferred energy without affecting the blocking probability too much. In particular, by controlling the total length of the idle zones I in **Layout-III**, we can achieve different DWC lanes with different road lengths and charging rates. In this subsection, we set $L = 10$ miles and $r = 50$ kW for **Layout-I**, and consider two specific layouts of **Layout-III**:

- **Layout-III-A:** $L = 10$ miles, $I = 5$ miles and equiva-

lent charging rate $r = 33.3$ kW.

- **Layout-III-B:** $L = 10$ miles, $I = 10$ miles and equivalent charging rate $r = 25$ kW.

Fig. 10 compares the performance metrics of **Layout-I**, **Layout-III-A** and **Layout-III-B**. Because different layouts adopt different average charging rate, for fair comparison, we transform the horizontal axis of the figures to available power capacity by multiplying the available capacity with its corresponding average charging rate. In addition, instead of comparing the average transferred energy, we turn to focusing on the average delivered energy (i.e., including the energy consumption due to driving). This change is to eliminate the influence from the power consumption of driving through the WPT-enabled roads because EVs drive through different distances in different layouts. In Fig. (10a), it can be observed that the blocking probabilities of the three layouts are close to each other especially in the light traffic cases, and the layout with longer length and lower charging rate has a relatively higher blocking probability. However, the average total power consumption and delivered energy per EV are increased by **Layout-III** as shown in Figs. (10b) and (10c). More importantly, the impact of **Layout-III** is larger in the slow speed regime. If we post a lower speed limit (e.g., 35 miles/hour as shown in the Fig. 10), **Layout-III-A** improves all the three performance metrics while **Layout-III-B** makes no difference. This means the performance gains by **Layout-III** are constrained by the lower speed limits. Therefore, given the lower speed limit of the DWC system, the total length of the idle zones I in **Layout-III** can be designed to optimize all the performance metrics. Furthermore, in the slow speed regime of the heavy traffic cases, we can clearly observe that trade-offs between the blocking probability and average delivered energy in the **Layout-III-A** and **Layout-III-B**. Thus, if the DWC system is allowed to operate in slow speed regime, the two QoS-related metrics can be controlled via admission control to achieve the target trade-offs.

By taking the characteristics of the three types of layouts into consideration, the DWC infrastructure planner can choose the layout as follows. *i*) If the EV traffic is predicted to stay in the light traffic case, or increase slightly, **Layout-III** should be chosen as long as the blocking probability can be guaranteed. In this case, a relatively low blocking probability can be guaranteed easily. Both high carried load and high average delivered energy can be achieved. Based on the predicted traffic and the lower speed limit, a proper length of the idle zone I should be determined by numerical evaluation to improve the carried load, and achieve the trade-offs between the blocking probability and average delivered energy per EV. *ii*) If the EV traffic is predicted to increase dramatically, **Layout-II** is chosen to guarantee the blocking probability. Moreover, each short lane of **Layout-II** can also adopt the concept of **Layout-III** based on the predicted traffic and lower speed limit.

5. CONCLUSIONS

This paper has modeled the DWC system as an $M/G/s/s$ state-dependent queue and evaluated its performance by a revenue-related metric (i.e., carried load), and QoS-related metrics (i.e., blocking probability and average transferred energy per EV). By analyzing the impact of the speed limit and the available capacity on the performance of the DWC system, we have shown the effectiveness of admission control and speed regulation in maximizing the system revenue with QoS guarantee. In addition, useful insights in choosing the long-term infrastructure parameters have been provided by comparing different layouts of the WPT-enabled road.

6. ACKNOWLEDGMENTS

The authors thank Mr. Yuxuan Jiang from the Hong Kong University of Science and Technology, for valuable and insightful discussions. The work presented in this paper was supported by the Hong Kong Research Grants Councils General Research Fund under Project 16209814 and Project 16210215.

7. REFERENCES

[1] M. D. Galus, M. G. VayÃą, T. Krause and G. Andersson, "The role of electric vehicles in smart grids," *Wiley Interdiscipl. Rev.: Energy Environ.*, 2(4), pp. 384-400, 2013.

[2] P. You, Z. Yang, M. Chow and Y. Sun, "Optimal cooperative charging strategy for a smart charging station of electric vehicles," *IEEE Trans. Power Syst.*, 31(4), pp. 2946-2956, 2015.

[3] P. Fan, B. Sainbayar, and S. Ren, "Operation analysis of fast charging stations with energy demand control of electric vehicles," *IEEE Trans. Smart Grid*, 6(4), pp. 1819-1826, 2015.

[4] X. Tan, B. Sun, D.H.K. Tsang, "Queueing Network Models for Electric Vehicle Charging Station with Battery Swapping," *in Proc. IEEE Int. Conf. Smart Grid Commun.*, Nov. 2014.

[5] A. Barkow, G. Campatelli, R. Barbieri, S. Persi, "Solutions and business models for wireless charging of electric vehicles," *in Electric Vehicle Business Models*, pp. 109-125, 2015.

[6] Highway England, "Feasibility study: powering electric vehicles on England's major roads," July 2015.

[7] J. Miller, P. Jones, J.-M. Li, and O. Onar, "ORNL experience and challenges facing dynamic wireless power charging of EVs," *IEEE Circuits and Systems Magazine*, 15(2), pp. 40-53, 2015.

[8] Y. D. Ko, Y. J. Jang, "The optimal system design of the online electric vehicle utilizing a wireless power transmission technology," *IEEE Trans. Intell. Transp. Syst.*, 14(3), pp. 1255-1265, Sep. 2013.

[9] F. Deflorio, L. Castello, I. Pinna, I. and P. Guglielmi, "Charge while driving for electric vehicles: road traffic modeling and energy assessment," *J. Mod. Power Syst. Clean Energy*, 3(2), pp.277-288, 2015.

[10] T. V. Theodoropoulos, I. G. Damousis, A. J. Amditis, "Demand-side management ICT for dynamic wireless EV charging," *IEEE Trans. Ind. Electron.*, 63(10), pp. 6623-6630, Oct. 2016.

[11] S. Ahn, J. Y. Lee, D. H. Choi, and J. Kim, "Magnetic field design for low EMF and high efficiency wireless power transfer system in on-line electric vehicles," *in Proc. CIRP Des. Conf.*, pp. 233-239, 2011.

[12] H. Xie, T. Ding, S. Liu and Z. Bie, "Sequential power flow simulation of integrated dynamic wireless power transfer systems," *in Proc. Power and Energy Society General Meeting*, 2016.

[13] C. Ou, H. Liang, and W. Zhuang, "Investigating wireless charging and mobility of electric vehicles on electricity market," *IEEE Trans. Industrial Electronics.*, 62(5), pp. 3123-3133, 2015.

[14] C. Kong and M. Devetsikiotis, "Optimal charging framework for electric vehicles on the wireless charging highway," *in Proc. CAMAD*, 2016.

[15] J.-C. Herrera, D. Work, R. Herring, J. Ban, Q. Jacobson, A. Bayen, "Evaluation of traffic data obtained via GPS-enabled mobile phones: the mobile century experiment," *Transp. Res. C*, 18(4), pp. 568-583, 2009.

[16] R. Jain, J. M. Smith, "Modeling vehicular traffic flow using M/G/C/C state dependent queueing models," *Transportation Science*, 31(4), pp. 324-336, 1997.

[17] J. Y. Cheah, J. M. Smith, "Generalized M/G/C/C state-dependent queuing models and pedestrian traffic flows", *Queueing Syst.*, 15(14), pp. 365-386, Mar. 1994.

[18] H. Wang, J. Li, Q. Chen, D. Ni, "Speed-density relationship: from deterministic to stochastic," *in Proc. Transp. Res. Board Annual Meeting*, Jan. 2009.

[19] M. Nikolic, M. Bierlaire, B. Farooq and M. de Lapparent, "Probabilistic speed-density relationship for Pedestrian traffic," *Transp. Res. B*, 89, pp. 58-81, 2016.

[20] A. Ingolfsson and L. Tang, "Efficient and reliable computation of birth-death process performance measures," *INFORMS J. Comput.*, 24(1), pp. 29-41, 2012.

[21] HK Electric, *Block Rate Tariff*, 2016, [Online]. Available: https://www.hkelectric.com/en/customer-services/billingpayment-electricity-tariffs/residential-tariff

[22] A. D. May, *Traffic Flow Fundamentals*, Prentice Hall, Englewood Cliffs, 1990.